

## MEASUREMENT OF CROSS SECTIONS AND THICK TARGET YIELDS FOR $(\alpha, \gamma)$ PROCESS ON $^{63}\text{Cu}$

I. CATA-DANIL<sup>1</sup>, M. IVASCU<sup>1</sup>, T. GLODARIU<sup>1</sup>, N. V. ZAMFIR<sup>1</sup>, D. BUCURESCU<sup>1</sup>,  
D. FILIPESCU<sup>1</sup>, G. CATA-DANIL<sup>1</sup>, L. STROE<sup>1</sup>, C. MIHAI<sup>1</sup>, D. GHITA<sup>1</sup>, G. SULIMAN<sup>1</sup>,  
T. SAVA<sup>1</sup>

<sup>1</sup> National Institute for Nuclear Physics and Engineering, P.O.Box MG-6,  
RO-077125 Bucharest-Magurele, Romania, E-mail: ivascu@tandem.nipne.ro

(Received June 27, 2008)

*Abstract.* We have measured the cross sections and the thick target yields for the  $^{63}\text{Cu}(\alpha, \gamma)^{67}\text{Ga}$  reaction in the 6.2 to 3.4 MeV, respectively 6 to 10 MeV, energy range using the activation technique. Natural copper was bombarded with an alpha beam delivered by the IFIN-HH Tandem accelerator. Irradiated samples were counted using a  $\gamma$ -spectrometry system low background facility. The characteristic activity of  $^{67}\text{Ga}$  was counted with a pair of large volume Ge detectors in close geometry to maximize the detection efficiency. The results are compared with statistical model prediction for different global  $\alpha$  particle potentials.

*Key words:* nucleosynthesis, cross section, yield.

### 1. INTRODUCTION

Nucleosynthesis studies of elemental evolution in a stellar environment use an extensive network of nuclear reactions, of which cross sections data for different nuclear reaction channels are important. Stable isotopes in the nuclear chart above iron are classified as  $s$ ,  $r$  and  $p$  nuclei, depending upon their Nucleosynthesis production processes. The  $s$ -isotopes are produced by the slow neutron capture process in stellar environments. The stable isotopes of the valley of stability in the nuclear chart are considered as being produced through the  $s$ -process. The  $r$ -isotopes are produced in high density neutron environments resulting from explosive stars and are located in the neutron rich side of the nuclear chart. The  $p$ -isotopes, the proton rich nuclei in the nuclear chart, have been identified to be produced through a sequence of photo-disintegration processes starting from some preexisting seed nuclei [1]. However, for experimental cross section measurements the common practice is to measure for example  $(p, \gamma)$  or  $(\alpha, \gamma)$  in the laboratory and to extract the cross section for the actual reaction of interest. Experimental data for

these reactions in the astrophysical relevant energy, *i.e.* at the sub-Coulomb barrier interaction energies near the Gamow window, are very scarce.

Anyhow, in recent years some  $\alpha$  capture cross sections on  $^{144}\text{Sm}$ ,  $^{70}\text{Ge}$ ,  $^{96}\text{Ru}$ ,  $^{112}\text{Sn}$  and  $^{63}\text{Cu}$  have been reported [2–6]. Most of the reported  $\alpha$ -capture data are found to be 2–5 times lower than the Hauser-Feshbach statistical model prediction. Improved global  $\alpha$ -optical potentials were proposed [7].

In addition to cross section data, thick target yields are used for astrophysical thermonuclear reaction rate derivations [8, 9] and also for cross section measurements [10, 11]. At sub-Coulomb barrier energies, where cross sections are usually very small, thick target yield measurement provide useful data on various important nuclear reactions.

In the present work, cross sections and thick target yield for  $\alpha$  induced reactions on  $^{63}\text{Cu}$  were measured.

## 2. EXPERIMENT

### 2.1. TARGET PREPARATION AND IRRADIATION OF $^{63}\text{Cu}$

Natural Cu foils of  $\sim 1.2\text{ mg/cm}^2$  thickness used in the experiment were prepared at the Legnaro National Laboratory. A stack of five  $^{nat}\text{Cu}$  targets and one  $^{nat}\text{Ti}$  foil of  $2.7\text{ mg/cm}^2$  thickness was prepared (see Table 1).

The beam current was  $\sim 0.1\text{ }\mu\text{A}$ . The incident  $\alpha$  beam energy on the successive foils was calculated based on the energy loss through Cu foils using  $dE/dx$  values estimated with TRIM code [18]. On average, the loss per Cu foil was about 550 keV.

The beam current was integrated using a special integrator. The titanium foil, at the end of the stack, was used for beam current calibration using the  $^{48}\text{Ti}(\alpha, n)^{51}\text{Cr}$  reaction and for catching the recoil  $^{67}\text{Ga}$  radio-isotopes from the preceding copper foil in order to estimate the recoiled fraction. More information

Table 1

Some of the irradiation conditions for the Cu targets with  $\text{He}^{++}$  beam

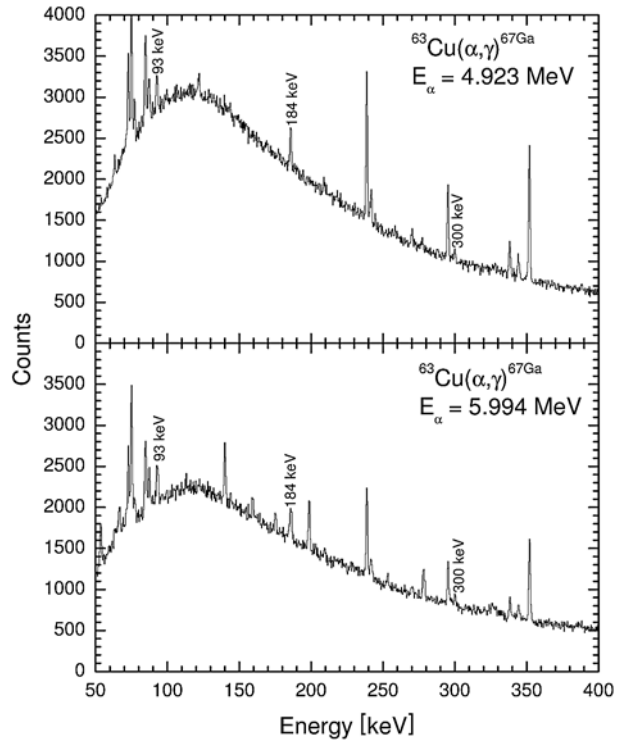
Sample	Thickness [ $\text{mg/cm}^2$ ]	Energy on the successive foils [MeV]	Current [nA]	Irradiation time [hours]
1	1.293	5.994	150	6
2	1.338	5.451	150	6
3	1.249	4.923	150	6
4	1.204	4.388	150	6
5	1.293	3.806	150	6

concerning the experimental setup and procedures can be obtained from our previous work [12].

## 2.2. DATA ACQUISITION AND ANALYSIS

Following the irradiation all the copper foils were counted for longer periods of time to measure the  $^{67}\text{Ga}$  activity using our counting setup (Fig. 3 [12]). The energy resolution of the HPGe detector was 1.9 keV at  $E_\gamma = 1332.5$  keV a partial HPGe  $\gamma$ -ray spectrum of  $^{67}\text{Ga}$  characteristic  $\gamma$  line ( $t_d$  and  $t_c$  are decay and counting times) is shown in Fig. 1. Efficiency calibration of the HPGe detectors was done using calibrated point sources (Fig. 5 [12]).

Fig. 1 – Partial HPGe  $\gamma$ -ray spectra of  $^{67}\text{Ga}$  characteristic  $\gamma$  lines.



The cross section were deduced from the well known activation equation:

$$A_0 = n\sigma\phi(1 - \exp(-\lambda t)), \quad (1)$$

where  $A_0 = ^{67}\text{Ga}$  activity at the end of irradiation (disintegration/s),  $n =$  number of  $^{63}\text{Cu}$  nuclei ( $\text{cm}^{-2}$ ),  $\sigma =$  cross section ( $\text{cm}^2$ ),  $\phi =$  number of incident  $\alpha$  particles ( $\text{s}^{-1}$ ) and  $(1 - \exp(-\lambda t)) =$  growth factor for a decay constant  $\lambda$  and irradiation time  $t$ .

The activity  $A_0$  at the end of irradiation was deduced from the measurement using the following equation:

$$A_0 = \lambda N_0 = \frac{\lambda C}{I_\gamma \epsilon (\exp - \lambda(t_{cs} - t_{ce}) - \exp - \lambda(t_{ce} - t_{ie}))}, \quad (2)$$

where  $N_0$  = number of  $^{67}\text{Ga}$  nuclei at the end of irradiation;  $t_{cs}$ ,  $t_{ce}$ ,  $t_{ie}$  = counting start, counting end and irradiation end, respectively;  $C$  = net area under the peak for a counting ( $t_{cs} - t_{ce}$ ) duration;  $I_\gamma$  =  $\gamma$  ray intensity;  $\epsilon$  = detector peak efficiency. Cross section for the  $^{63}\text{Cu}(\alpha, \gamma)^{67}\text{Ga}$  reaction reported in this paper are deduced using the 184 keV  $\gamma$  ray.

Titanium foil was counted after seven days. Recoiled  $^{67}\text{Ga}$  activity was determined using Eq. 1 and Eq. 2 and was found to be about 12% in this experiment. Assuming an uniform  $^{67}\text{Ga}$  recoil out at the successive foils in the stack, a correction of 12% of the  $^{67}\text{Ga}$  activity was made for the first Cu foil.

Measured cross section of  $^{48}\text{Ti}(\alpha, n)^{51}\text{Cr}$  reaction were compared with the published experimental data [13] for beam current calibration. Considering all uncertainties of detector efficiency calibration, target foil thickness, beam current, counting statistics, decay rate, and recoil fraction, we appreciate 18% uncertainties for the measured cross sections.

### 3. RESULTS AND DISCUSSION

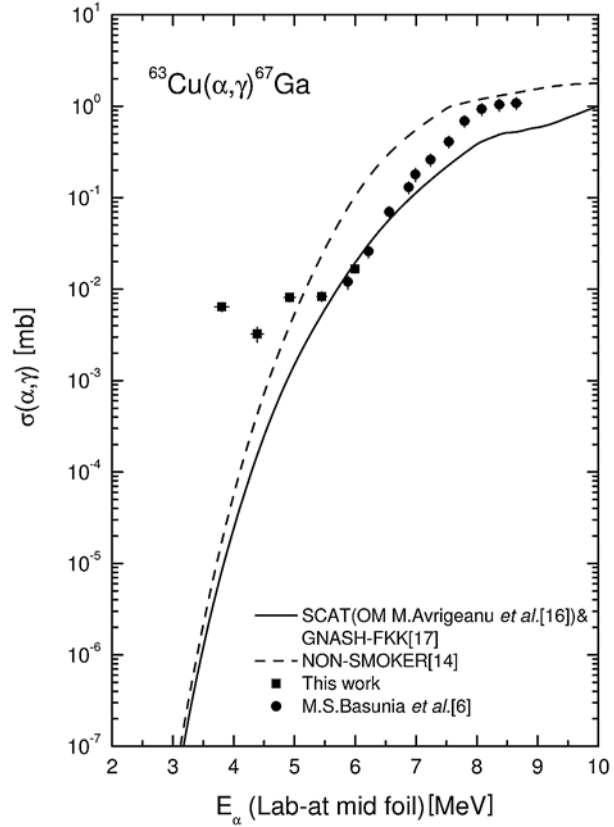
Measured cross section and  $S$  factors for the  $^{63}\text{Cu}(\alpha, \gamma)^{67}\text{Ga}$  reaction are presented in Table 2. In Fig. 2, measured values of cross section are presented along with the theoretical values of the Non-Smoker [14] and Gnash-FKK [17] statistical model codes. In Gnash-FKK estimation, the optical model potential of M. Avrigeanu *et al.* [16] for  $\alpha$  particles was used. From Fig. 2, it can be seen that the agreement between the experimental and theoretical data are reasonable good for the  $^{63}\text{Cu}(\alpha, \gamma)^{67}\text{Ga}$  reaction cross section even in the energy range (6.0–3.8) MeV.

Table 2

Measured cross section and astrophysical  $S$  factors of the  $^{63}\text{Cu}(\alpha, \gamma)^{67}\text{Ga}$  reaction

$E_{beam}$ (MeV)	$E_{cm}$ (MeV)	$\sigma$ ( $\mu\text{b}$ )	$S$ factor ( $10^{21}$ keV b)
$3.806 \pm 0.116$	$3.578 \pm 0.1088$	$6.408 \pm 0.7339$	$831.910 \pm 754.026$
$4.388 \pm 0.1014$	$4.126 \pm 0.0953$	$3.229 \pm 0.6029$	$8.489 \pm 6.1839$
$4.923 \pm 0.0916$	$4.629 \pm 0.0861$	$8.130 \pm 0.8688$	$1.120 \pm 0.5593$
$5.451 \pm 0.0823$	$5.125 \pm 0.0774$	$8.327 \pm 1.0329$	$0.097 \pm 0.0399$
$5.994 \pm 0.0655$	$5.636 \pm 0.0616$	$16.60 \pm 14.775$	$0.022 \pm 0.0068$

Fig. 2 – Comparison between experimental and theoretical cross section for the  $^{63}\text{Cu}(\alpha, \gamma)^{67}\text{Ga}$  reaction (see text for details).



A comparison of our experimental results with those of M. S. Basunia *et al.* [6] was made. Their reasonably good agreement provides an indication of the experimental integrity for the reported  $^{63}\text{Cu}(\alpha, \gamma)^{67}\text{Ga}$  cross-section measurement.

Based on the experimental cross section values from Table 2 we calculate the astrophysical S factor, using the following equation:

$$S(E) = \sigma(E) E \exp(2\pi\eta), \quad (3)$$

where  $\eta$  is the Sommerfeld parameter,  $\sigma(E)$  the cross section in the center of mass. These values are compared with those obtained by calculation using Non-Smoker code [3]. Based on Eq. 1, the thick target yield  $Y(E)$ , the equation for fully stopped beam in the target is the following:

$$Y(E) = n \int_0^E \frac{\sigma(E')}{(-dE'/dx)} dE' = \frac{A_0}{\phi(1 - \exp(-\lambda t))}, \quad (4)$$

where  $E$  is the incident energy,  $\sigma(E')$  is the energy dependent cross section, and  $dE'/dx$  is the stopping power.

Fig. 3 si 4

The yield for  $^{63}\text{Cu}(\alpha, \gamma)^{67}\text{Ga}$  reaction is calculated using Eq. 4 and considering successive thin slices of 1000 Å thickness. The incident energy on each of these conceptual targets is obtained using  $dE/dx$  from TRIM code [18]. The corresponding cross section is taken from a smooth fit mode to the theoretical data from [14]. The consideration of conceptual target layers continued until the incident beam energy reached zero. The number of target nuclei,  $n$ , is calculated for the 1000 Å thickness using the Avogadro's number, elemental mass, and pure isotopic abundance in target material. Finally, all thin target cross sections are summed to obtain the calculated yield in the energy range from (6–10) MeV shown in Fig. 4.

The result obtained by M. S. Basunia *et al.* [15] at 7 MeV bombarding energy is also presented. Theoretical calculation with Non-Smoker model [14] and Gnash-FKK model [17] using optical model potential of M. Avrigeanu *et al.* [16] are shown. It appears that the theoretical calculations of  $(\alpha, \gamma)$  yields are in reasonably good agreement with the experimental data.

*Acknowledgements.* The authors thank Mr. Manente (Legnaro National Laboratories) for the  $^{nat}\text{Cu}$  target preparation. We acknowledge the Tandem operational team of IFIN-HH for their help in performing the irradiation. This work was performed under the auspices of the Romanian Agency of Research under contract CEX-05-D11-50.

## REFERENCES

1. S. E. Woosely, W. M. Howard, *Astrophys. J. Suppl.*, **36**, 285 (1978).
2. E. Somorgai *et al.*, *Nucl. Phys.*, **A261**, 293c (1997).
3. Zs. Fülöp *et al.*, *Z. Phys.*, **A355**, 203 (1996).
4. W. Rapp *et al.*, *Phys. Rev.*, **C66**, 015803 (2002).
5. N. Özkan *et al.*, *Nucl. Phys.*, **A710**, 469 (2002).
6. M. S. Basunia *et al.*, *Phys. Rev.*, **C71**, 035801 (2005).
7. P. Demetriou, C. Grama, S. Goriely, *Nucl. Phys.*, **A707**, 253 (2002).
8. N. A. Doughton *et al.*, *At. Data Nucl. Data Tables*, **23**, 177 (1979).
9. N. A. Doughton *et al.*, *At. Data Nucl. Data Tables*, **28**, 341 (1983).
10. E. B. Norman, T. E. Chupp, K. T. Lesko, *Astrophys. J.*, **231**, 834 (1981).
11. F. K. Mc Gowan *et al.*, *Phys. Rev.*, **133**, B 907 (1964).
12. I. Cata-Danil *et al.*, *Rom. Rep. Phys.*, **59**, 197 (2007).
13. A. J. Morton *et al.*, *Nucl. Phys.*, **A537**, 167 (1992).
14. T. Rauscher and F.-K. Thielemann, *At. Data Nucl. Data Tables*, **79**, 47 (2001).
15. M. S. Basunia *et al.*, *Phys. Rev.*, **C75**, 015802 (2007).
16. M. Avrigeanu *et al.*, *Nucl. Phys.*, **A723**, 104 (2003).
17. P. G. Young, E. D. Arthur, M. B. Chadwick, Gnash-FKK code, PSR-125, RSIC-ORNL, 1996.
18. J. F. Ziegler, J. P. Biersack, U. Littmark, *The Stopping and Range of Ions in Solids*, Pergamon Press, New York, 1985.



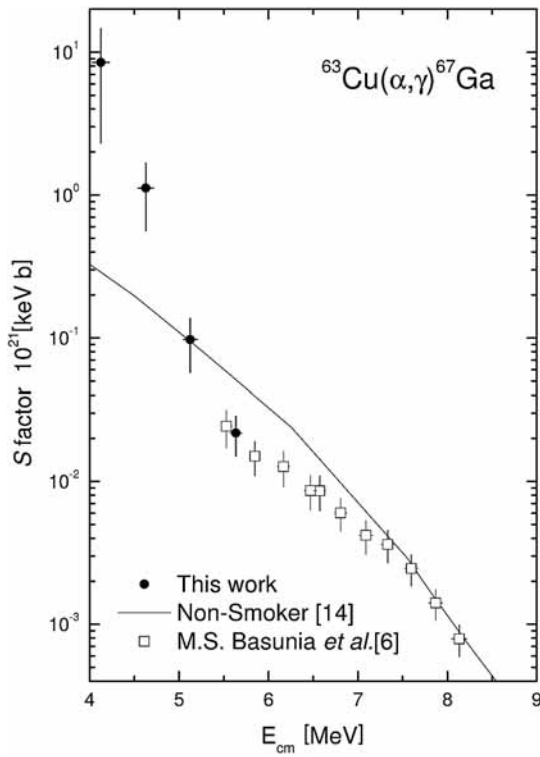


Fig. 3 – Astrophysical  $S$  factors calculated for the  $^{63}\text{Cu}(\alpha, \gamma)^{67}\text{Ga}$  reaction.

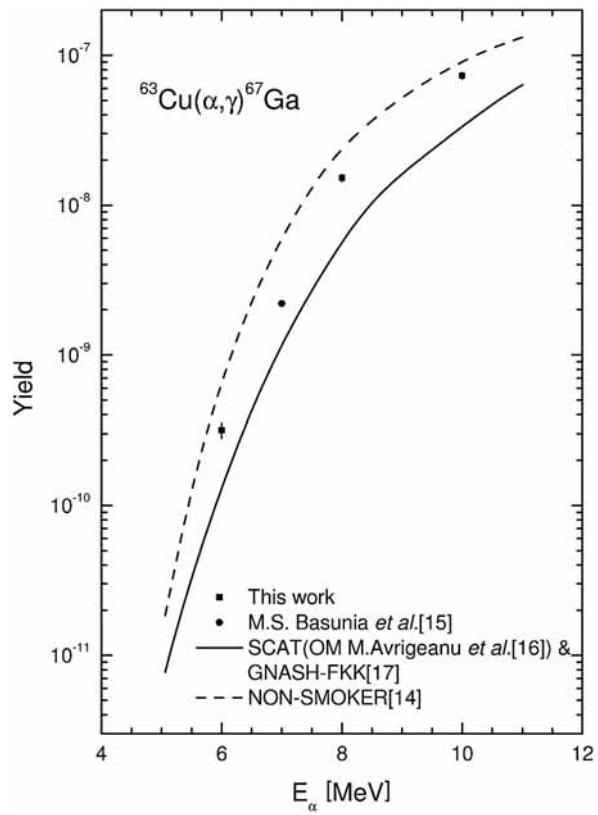


Fig. 4 – Experimental and calculated yield for the  $^{63}\text{Cu}(\alpha, \gamma)^{67}\text{Ga}$  reaction (see text for details).